Structure and magnetism of homometallic ludwigites: $Co_3O_2BO_3$ versus $Fe_3O_2BO_3$

D. C. Freitas, M. A. Continentino,* R. B. Guimarães, and J. C. Fernandes
Instituto de Física, Universidade Federal Fluminense, Campus da Praia Vermelha, 24210-340, Niterói, RJ, Brazil

J. Ellena
Instituto de Física de São Carlos, Universidade de São Paulo, Caixa Postal 369, 13560-970, São Carlos, SP, Brazil

L. Ghivelder
Instituto de Física, Universidade Federal do Rio de Janeiro, Caixa Postal 68528, 21945-970, RJ, Brazil
(Received 7 January 2008; revised manuscript received 7 April 2008; published 20 May 2008)

We present an extensive study of the structural, magnetic, and thermodynamic properties of the oxyborate $Co_3O_2BO_3$. This is carried out through x-ray diffraction, static and dynamic magnetic susceptibilities, and specific heat experiments in single crystals in a large temperature range. The structure of $Co_3O_2BO_3$ is composed of subunits in the form of three-leg ladders where Co ions with mixed valency are located. The magnetic properties of this Co *ludwigite* are determined by a competition between superexchange and double-exchange interactions in the low-dimensional subunits. We discuss the observed physical properties in comparison with the only other known homometallic ludwigite, $Fe_3O_2BO_3$. The latter presents a structural distortion in the ladders and two magnetic transitions. Both features are not found in the present study of the Co ludwigite. The reason for these differences in the structural and magnetic behavior of two apparently similar compounds is discussed.

DOI: 10.1103/PhysRevB.77.184422 PACS number(s): 75.20.Ck, 73.50.Fq

I. INTRODUCTION

The anhydrous oxyborates of the 3*d* transition metals form mainly in the warwickit and ludwigite structures in which boron ions have triangular coordination. They possess instigating magnetic and structural properties[1,2] among which it is worth noting the structural transition of the iron ludwigite $Fe_3O_2BO_3$ (Ref. 3). This transition, to which the attention of several researchers has been recently called, consists of a zigzag transformation of the iron columns of trivalent ions inside three-leg ladders (3LLs). It starts at 283 K, going to low temperatures, and it is commensurate with the lattice. At 112 K the trivalent iron ions in 3LLs are magnetically ordered, but only at 70 K is the whole ensemble of divalent and trivalent ions ordered.[4–6] At present there are three theories for explaining this behavior, but none of these fully explains all its features.[7–9]

In order to better understand these transitions, we decided to study, as a function of temperature, the structural and magnetic properties of the *only* other known homometallic ludwigite. This is the cobalt ludwigite whose chemical formula is $Co_3O_2BO_3$. It was known[10] that its crystalline structure has the same space group with nearly the same lattice parameters of the iron system at room temperature (RT). Also transition metals have one trivalent and two divalent ions per chemical formula in both compounds as shown in Sec. II B. These similarities suggest of course similar behaviors. These ludwigites are said to be *homometallic* since all the metal ions in each compound are of the same chemical element. The present work adds to previous studies of this material by Huang *et al.*[11] and by Ivanova *et al.*[12] a detailed low-temperature structural analysis using x-ray diffraction. Furthermore, we present specific heat results in a large temperature range and ac-magnetic-susceptibility measurements.

For the above-mentioned study, we have synthesized high-quality single crystals of $Co_3O_2BO_3$ for obtaining clear measurements of the relevant physical properties. ac magnetic susceptibility, dc magnetization, and specific heat under magnetic fields up to 9 T were measured between 2 K and RT. Also x-ray diffraction in single crystals has been performed so that their crystalline structure could be completely solved at RT and at 105 K. Besides, these latter experiments confirmed the excellent quality of the crystals. As a general result, we found that the physical properties of both oxyborates are quite distinct. The cobalt ludwigite has only one magnetic critical temperature instead of the two magnetic transitions observed in the Fe system. The present material is fully ordered at T_N=42 K. Also, we have not found any structural transition in the Co ludwigite in contrast to the iron system. It remains a challenging problem to understand accurately the reason for the different physical behavior of these ludwigites and for the existence of the structural transition in the iron material.

II. EXPERIMENT

A. Sample preparation

The crystals of $Co_3O_2BO_3$ have been synthesized in two steps as suggested by Rowsell *et al.*[13] First, a 3:1 molar mixture of $CoCO_3 \cdot x(H_2O)$ and H_3BO_3, calculated as if the carbonate does not contain any water, was fired at 1100 °C in air for 24 h and slowly cooled. In a second step the product of the first reaction was mixed with borax ($Na_2B_4O_7$) and fired again at 1100 °C for 12 h and slowly cooled. The final product contained prismatic and octahedral crystals of $Co_3O_2BO_3$ and Co_3O_4, respectively. After washing, the former were manually separated under a microscope. They measured about 0.8 mm in length. An x-ray analysis of some of these crystals revealed the absence of any structural disorder or crystalline domains.

B. X-ray diffraction

A black prism-shaped crystal of dimensions 0.420 $\times 0.183 \times 0.161$ mm^3 was used for data collection from x-ray diffraction. The measurements were carried out on an Enraf-Nonius Kappa-CCD diffractometer with graphite monochromatic Mo Kα radiation ($\lambda = 0.710\,73$ Å). Low-temperature measurements were made using an Oxford Cryosystem device. The cell refinements were performed using the softwares COLLECT[14] and SCALEPACK.[15] The final cell parameters were obtained on all reflections. Data were collected up to 62.0° in 2θ. Data reduction was carried out using the software DENZO-SMN, SCALEPACK, and XDISPLAYF[15] for visual representation of the data. A Gaussian absorption correction was applied.[16] The structure was solved using the software SHELXS-97[17] and refined using the software SHELXL-97.[18] All atoms were clearly solved and full-matrix least-squares refinement procedures on F^2 with anisotropic thermal parameters were carried out using SHELXL-97. Crystal data, data collection parameters, and structure refinement data are summarized in Table I. Tables were generated by WINGX.[19] Other softwares were also used in order to publish the crystal data such as ORTEP-3[20] and DIAMOND 3.1 by Bergerhoff *et al.*[21]

The unit cell parameters were determined at several temperatures between RT and 105 K. This procedure did not show any evidence of some phase transition as found in the iron ludwigite. Even so we decided to perform a structure determination at 293 K and 105 K to compare both crystal structures, in analogous experimental conditions, in order to see if there was any conformational change with temperature. No conformational change was observed. Therefore, hereinafter, all discussion is given in terms of the RT structure.

Figure 1 shows the structure of $Co_3O_2BO_3$ projected along the c axis together with the polyhedra centered at Co ions. Figure 2 shows an ORTEP-type view of the asymmetric unit plus the coordination environment around Co ions. Some selected geometric parameters are shown in Table II. The mean B-O bond length and the mean O-B-O bond angle are in good agreement with the expected trigonal planar geometry. It is important to note that the coordinations around the Co(1), Co(2), and Co(3) sites are distorted octahedra. The Co-O bond lengths range from 2.006(2) Å to 2.148(1) Å for Co(1), from 1.996(2) Å to 2.118(1) Å for Co(2), and from 2.054(2) Å to 2.138(1) Å for Co(3). The coordination bond lengths seem to be more homogeneous around Co(4).

The space group of $Co_3O_2BO_3$ is the same as that found for the ludwigite $Fe_3O_2BO_3$ at RT with comparable cell parameters.[3] The structure of $Co_3O_2BO_3$ also presents a trinuclear metal cluster (triad) like that found in the Fe compound now formed by Co(4)-Co(2)-Co(4) ions. These clusters form columns along the c axis (3LL), shown in Fig. 3, in which the Co(4)-Co(2) bond length is equal to 2.7510(4) Å. We remark that in $Fe_3O_2BO_3$ the corresponding lenght[3] is 2.786(1) Å. The space group we obtain is the same found in Refs. 10–12. The room-temperature lattice parameters are very similar to those found in these references.

From the Co-O distances given in Table II, we may find the oxidation numbers for the Co ions in each lattice site. We use the formulas given by Wood and Palenik[22] for the oxidation number Z_j for the Co ion on site j,

$$Z_j = \sum_i s_{ij}, \tag{1}$$

where $s_{ij} = \exp[(R_0 - r_{ij}/b\,]$, with r_{ij} the distance to the nearest-neighbor oxygen ions. R_0 and b are parameters given in Ref. 22 for inorganic cobalt compounds. The results for the oxidation numbers Z_j are given in Table III. They show that we can nominally ascribe valence 2^+ for Co ions on sites 1, 2, and 3 and valence 3^+ for Co ions on site 4.

TABLE I. Crystal data and structure refinement.

Empirical formula		$Co_6B_2O_{10}$
Formula weight		535.20
Wavelength		0.717073 Å
Crystal size		$0.420 \times 0.183 \times 0.161$ mm^3
Temperature	293(2) K	105.0(1) K
Crystal system	Orthorhombic	Orthorhombic
Space group	*Pbam*	*Pbam*
Unit cell dimension a=	9.3041(3) Å	9.3014(3) Å
b=	11.9414(4) Å	11.9317(4) Å
c=	2.9627(1) Å	2.95870(1) Å
Volume	329.168(19) Å^3	328.361(19) Å^3
Z	2	2
Density (calculated)	5.400 Mg/m^3	5.413 Mg/m^3
Absorption coefficient	14.824/mm	14.861/mm
F(000)	504	504
θ range (deg)	3.41°–31.00°	3.41°–31.00°
Index range h=	−13, 13	−13, 13
k=	−17, 17	−17, 17
l=	−4, 3	−4, 3
Reflections collected	2681	2780
Independent reflections	615	611
R(int)	0.0441	0.0592
Completeness to θ=31.01	99.5%	99.0%
Absorption correction	Gaussian	Gaussian
Max/min transmission	0.139/0.045	0.142/0.048
Refinement method: Full-matrix least squares on F^2		
Data/restraints/parameters	615/0/58	611/0/54
Goodness of fit on F^2	1.210	1.231
Final R indices [$I > 2\sigma(I)$]	$R1 = 0.0294$	$R1 = 0.0361$
	$wR2 = 0.0685$	$wR2 = 0.0851$
R indices (all data)	$R1 = 0.0298$	$R1 = 0.0366$
	$wR2 = 0.0689$	$wR2 = 0.0857$
Extinction coefficient	0.36(1)	0.437(2)
Largest diff. peak	1.277e Å^{-3}	1.416e Å^{-3}
Largest diff. hole	−1.787e Å^{-3}	−2.951e Å^{-3}

III. MAGNETIC PROPERTIES

We have performed a detailed investigation of the magnetic properties of the Co ludwigite system, using a commer-

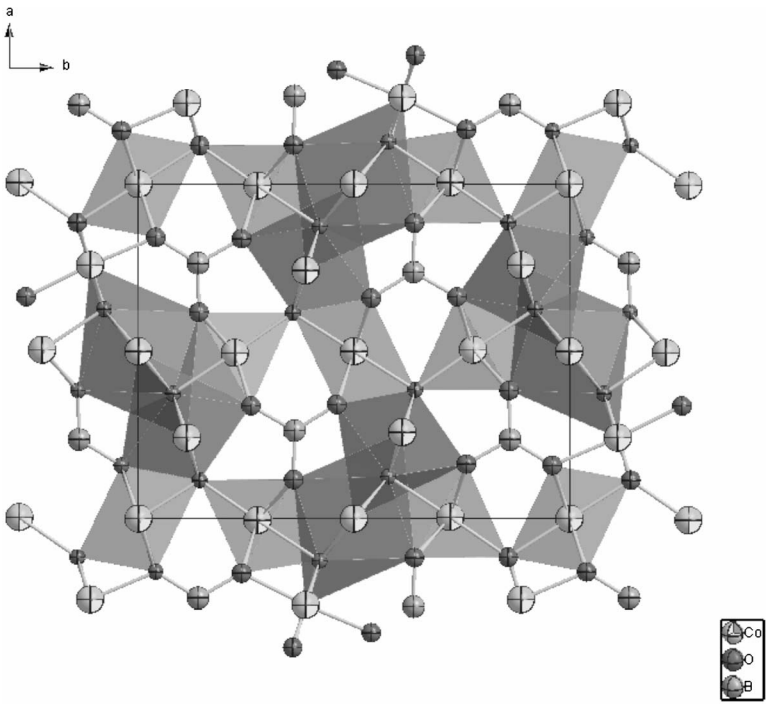

FIG. 1. The structure of $Co_3O_2BO_3$ projected along the c axis, together with the polyhedra centered on the Co atoms. The lines indicate side a and b axes of the unit cell. The dark polyhedra contain the metal sites Co(2) and Co(4) as shown in Fig. 3.

cial PPMS platform (Quantum Design). As pointed out before, due to small differences in the magnetic moments and lattice parameters, we expected to find similar behavior to that of the Fe system. Figure 4 shows the inverse dc susceptibility ($\chi_{dc}^{-1}=H/M$) measured as a function of temperature in an applied magnetic field of 1 T. From this figure we can determine the Curie-Weiss temperature $\theta_{CW}=-25$ K, which indicates the predominance of antiferromagnetic interactions in the system. The Curie-Weiss temperature[3] of $Fe_3O_2BO_3$ is $\theta_{CW}=-485$ K. Although this is nearly 20 times that of the Co ludwigite, the ordering temperatures differ by a factor less than 2, as we show below.

The effective moment per Co atom obtained from the Curie-Weiss constant given by Fig. 4 is $p=g\sqrt{J(J+1)}=4.16$, which yields $J=1.64$. The average moment per unit cell with two divalent ($S=3/2$) and one trivalent ($S=2$) Co ions is given by $\bar{S}=[2(3/2)+2]/3=1.66$, where we neglected the orbital contribution.

Figure 5 shows ac-susceptibility measurements for different frequencies as a function of temperature. The real part of χ_{ac} shows a sharp peak at the temperature $T_N=42$ K, which we identify as the Néel temperature of the material. There is no frequency dependence of T_N, which implies that this is a well-defined thermodynamic transition as confirmed by specific heat results to be shown later. The imaginary part of χ_{ac}, but not the onset of dissipation, shows a frequency dependence as expected from the formation of domain walls in the ordered magnetic phase.

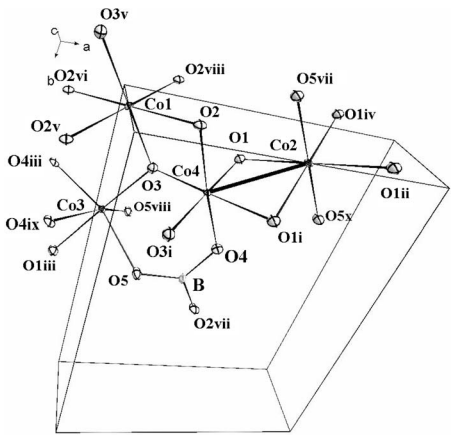

FIG. 2. ORTEP-type view of the structure fragment of ludwigite. Ellipsoids are drawn at the 60% probability level. Symmetry codes: (i) $x, y, -1+z$; (ii) $1-x, -y, -1+z$; (iii) $-0.5+x, 0.5-y, 1-z$; (iv) $1-x, -y, z$; (v) $-x, -y, z$; (vi) $-x, -y, 1+z$; (vii) $0.5-x, 0.5+y, -z$; (viii) $x, y, 1+z$; (ix) $-0.5+x, 0.5-y, -z$; (x) $0.5+x, 0.5-y, -z$; (xi) $-x, 1-y, -1+z$; (xii) $-1+x, y, z$.

TABLE II. Selected bond lengths in Å. For symmetry codes, see Fig. 2.

Co(1)-O(2)	2.148(1)	B-O(5)	1.361(4)
Co(1)-O(3)	2.006(2)	B-O(2)^{vii}	1.377(4)
Co(2)-O(1)	2.118(1)	Co(2)-Co(3)	3.0539(4)
Co(2)-O(5)^{vi}	1.996(2)	Co(2)-Co(4)	2.7510(4)
Co(3)-O(1)^{iii}	2.054(2)	Co(3)-Co(4)	3.0868(5)
Co(3)-O(3)	1.951(2)	Co(1)-Co(1)^{viii}	2.9627(1)
Co(3)-O(5)	2.113(1)	Co(1)-Co(1)^{xi}	3.0092(3)
Co(3)-O(4)^{iii}	2.138(1)	Co(2)-Co(2)^{i}	2.9627(1)
Co(4)-O(1)	1.963(1)	Co(3)-Co(3)^{i}	2.9627(1)
Co(4)-O(2)	1.974(2)	Co(3)-Co(2)^{viii}	3.0539(4)
Co(4)-O(3)^{i}	1.928(1)	Co(4)-Co(1)^{xii}	3.0092(3)
Co(4)-O(4)	1.983(2)	Co(4)-Co(3)^{i}	3.0868(5)
B-O(4)	1.387(4)	Co(4)-Co(4)^{i}	2.9627(1)

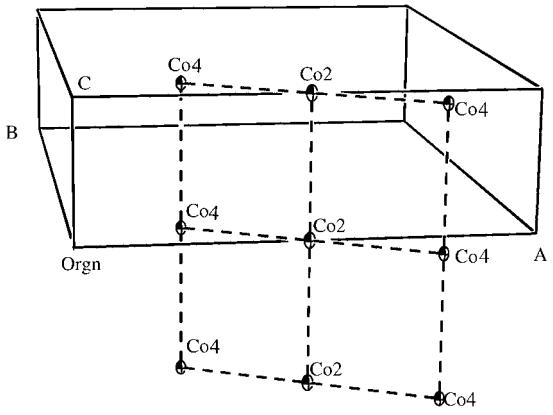

FIG. 3. Trinuclear cluster columns of metal sites (3LLs) along the crystallographic c axis and its relative position with respect to the unit cell (solid lines).

Further static magnetic measurements presented in Figs. 6 and 7 confirm the temperature of the magnetic transition and clarify the nature of this transition as that to a weak ferromagnetic or ferrimagnetic state. This is indicated by the presence of a spontaneous magnetization found in field-cooling and zero-field-cooling procedures. In zero-field cooling the ordered magnetic system breaks down in magnetic domains, as evidenced by the drop in the magnetization curves and consistent with the observation of dissipation in χ''_{ac} below T_N. Notice in Fig. 6 that in small fields ($H=100$ Oe), the transition is very sharp, almost suggesting a first-order instability. This is ruled out, however, by the absence of any hysteresis in the field-cooling (FC) and zero-field-cooling (ZFC) procedures for $T \geq T_N$. For moderate fields ($H=0.1$ T) the transition is still sharp, becoming smooth only for fields of the order of 1 T. Notice that the magnetic transition temperature T_N is field independent. This will be further confirmed by the specific heat measurements presented below.

The magnetic transition observed at $T_N \approx 42$ K is in agreement with the results of Ivanova *et al.*[12] However, these authors report a second magnetic transition at lower temperatures (~ 17 K) which is not found in the present work, neither in magnetic nor thermodynamic experiments. A possible explanation for this discrepancy is the existence of a spurious phase in Ref. 12. They also report electrical transport measurements well above the magnetic transition.

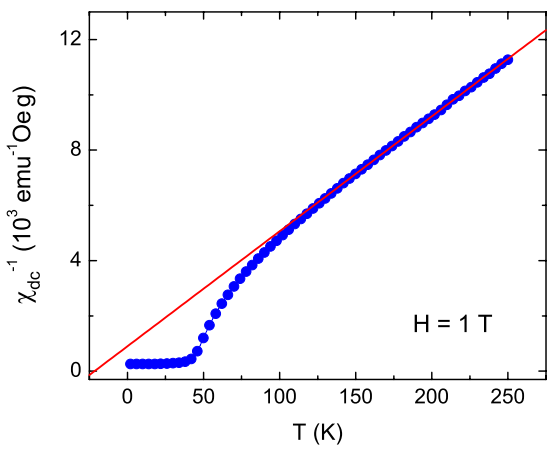

FIG. 4. (Color online) Inverse magnetization of the Co ludwigite in a 1-T magnetic field. The paramagnetic Curie-Weiss temperature is $\theta_{CW}=-25$ K.

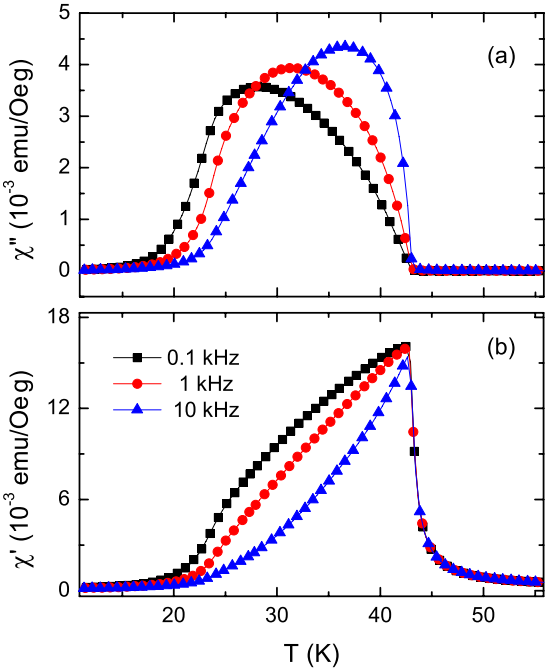

FIG. 5. (Color online) Real (χ') and imaginary (χ'') parts of the ac susceptibility of $Co_3O_2BO_3$ for different frequencies.

At this point let us recall that in the Fe ludwigite two magnetic transitions were observed.[3] The one at higher temperatures (112 K) did not show up in the dynamic and static magnetic measurements, the same that we have presented above for the Co system. However, Mössbauer spectroscopy

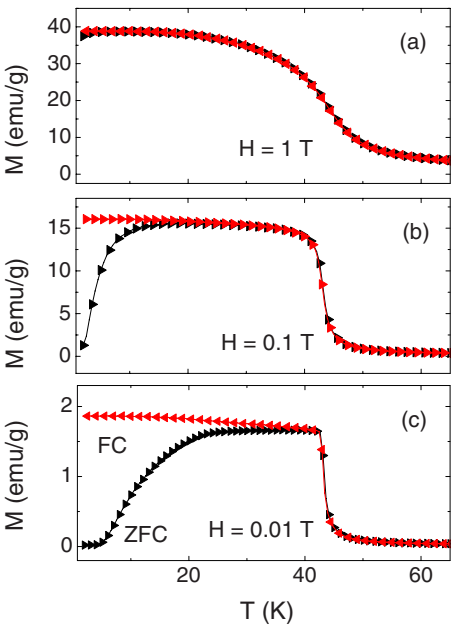

FIG. 6. (Color online) Static magnetization of $Co_3O_2BO_3$ in FC and ZFC procedures for several external magnetic fields.

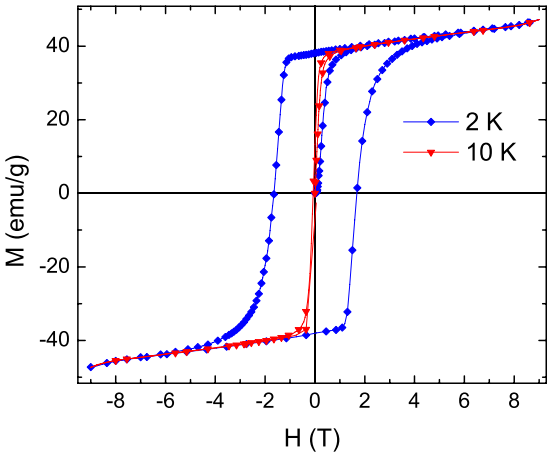

FIG. 7. (Color online) Hysteresis cycle of $Co_3O_2BO_3$ magnetization at 2 K and 10 K.

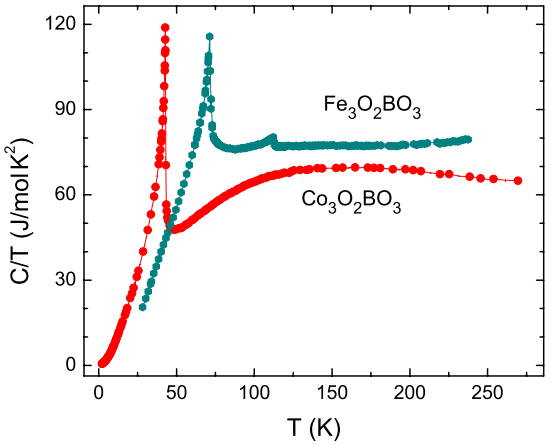

FIG. 8. (Color online) Specific heat as a function of temperature for the Fe and Co ludwigites. In the Fe system there are two magnetic transitions (Ref. 23), while in the Co material there is a single transition. These transitions appear as anomalies in the specific heat curve.

and later on specific heat results have clearly shown the existence of this partial magnetic transition due to the ordering of Fe moments along the three-leg ladders. Only at lower temperatures (T_N=70 K) does the whole system of Fe moments become magnetically ordered, with now clear signatures in the dynamic and static susceptibilities. The latter is the same type of magnetic transition, involving all magnetic ions, which we actually observe in the Co material. In this Co system, however, there is no partial ordering at higher temperatures. Although we cannot count with the information of Mössbauer experiments in the present case, the existence of a single magnetic transition is confirmed by specific heat measurements to be presented below.

The absence of partial magnetic ordering along the 3LLs for $T > T_N$ in $Co_3O_2BO_3$ clearly correlates with the absence of a dimerization transition in this system. Here dimerization means a structural transitions which approximates two cations and can be observed by x-ray scattering. For completeness, we present in Fig. 7 magnetization versus field data for $Co_3O_2BO_3$ at low temperatures (2 and 10 K), *much* below T_N. The existence of a remnant magnetization confirms the weak ferromagnetic or ferrimagnetic ordering of the moments. The moment obtained from the magnetization curve at the lowest temperature (T=2 K), $M = g\mu_b \bar{S}$, corresponds to an average spin $\bar{S}$=1.64, similar to that obtained above from the Curie-Weiss susceptibility ($\bar{S}$=1.66). It is worth pointing out that this magnetization in $Co_3O_2BO_3$ is at least one order of magnitude larger than that of the Fe material.[4]

TABLE III. Oxidation numbers for the cobalt ions in $Co_3O_2BO_3$ obtained by the method of Wood and Palenik (Ref. 22) from the distances appearing in Table II (see text).

Site	Oxidation number (Z_j)
Co(1)	1.913
Co(2)	2.056
Co(3)	1.977
Co(4)	2.725

This indicates that ferromagnetic interactions are more important in the former system. The appearance of a hysteresis cycle only occurs at the lowest temperature measured. This implies that the domain walls are quite mobile and only at these very low temperatures do they get pinned.

We have also carried out superconducting quantum interference device (SQUID) magnetometry measurements (not shown) in a single crystal on different orientations. These results are similar to those obtained in the extraction magnetometer (PPMS). They are useful to establish the direction perpendicular to the axis sample as the easy magnetization direction. We point out that neutron scattering[6] in $Fe_3O_2BO_3$ has shown that the moments in this compound are ordered perpendicular to the crystal c axis.

IV. SPECIFIC HEAT MEASUREMENTS

The absence of a microscopic probe to rule out a partial ordering magnetic transition in the Co ludwigite, differently from the Fe system, can be circumvented by specific heat measurements. The results were obtained with an ensemble of crystals, with a total mass of 5 mg, glued together with varnish. The measurements were made with and without an applied magnetic field by the relaxation technique, using the PPMS platform.

Figure 8 shows specific heat measurements for $Co_3O_2BO_3$ plotted with previous results for $Fe_3O_2BO_3$ (Ref. 23). In the Fe case two features are clearly observed which have been identified with two magnetic transitions. The one at higher temperatures is due to partial ordering of the Fe moments along the 3LLs as confirmed by Mössbauer spectroscopy[4,5] and neutron scattering.[6] The low-temperature feature at T_N =70 K marks the onset of magnetic ordering in the whole system. The Co ludwigite presents only the latter transition. There is no partial ordering in this system. The Néel temperature T_N=42 K obtained from the specific heat measurements coincides with that obtained from the static and dynamic magnetic measurements. Notice, as we pointed out

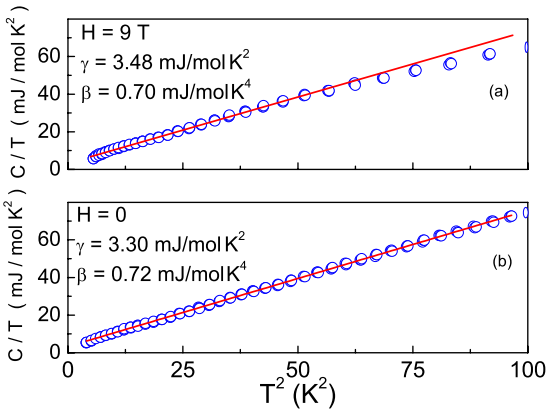

FIG. 9. (Color online) Low-temperature specific heat for the Co ludwigite plotted as C/T versus T^2 for (a) $H=9$ T and (b) $H=0$. The linear behavior shows the temperature region where the data are well described by the expression $C/T=\gamma+\beta T^2$. The values of γ and β for each field are shown in the figure.

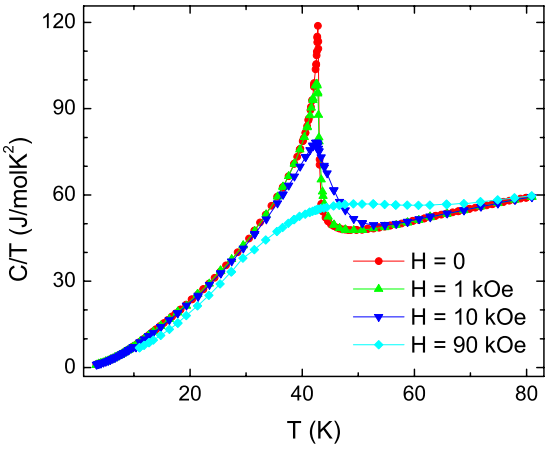

FIG. 10. (Color online) Specific heat as a function of temperature for the Co ludwigite in different applied magnetic fields.

before, that the Néel temperatures of the two ludwigites are not so different as expected from their different Curie-Weiss temperatures. Since the high-temperature magnetic measurements provide some average of the magnetic interactions, we interpret this result as another indication of the predominance of *ferromagnetic interactions* in the Co ludwigite, but it could also be attributed to frustration in the Fe system.

Below T_N, at the lowest measured temperatures, the specific heat exhibits a temperature dependence which is described by power laws. Figures 9(a) and 9(b) show the fitting by $C/T=\gamma+\beta T^2$ for a magnetic field of 9 T and in zero field. The T^3 term in solids is generally due to lattice excitations. In magnetic solids as antiferromagnetic or ferrimagnetic materials, it can also arise from spin waves with a linear dispersion relation. The origin of this contribution can be clarified by comparing the specific heat results in $H=0$ and $H=9$ T. The latter field should significantly *quench* the magnetic excitations below a temperature $T_Q=(g\mu_B\bar{S}H)/k_B\approx 20$ K for $\bar{S}=1.64$ as found before. In Fig. 9 the results of the fits yield a value for the coefficient γ with a small field dependence, $\gamma(H=0)=3.30$ mJ/(mol K^2) and $\gamma(H=9$ T$)=3.48$ mJ/(mol K^2). For the coefficients of the T^3 term they yield $\beta(H=0)=0.72$ mJ/(mol K^4) and $\beta(H=9$ T$)=0.70$ mJ/(mol K^4), in zero and 9 T magnetic fields. From these coefficients we can extract effective Debye temperatures θ_D, using $\theta_D=234R/\beta$ where R is the universal gas constant.[24] From the values of the coefficients β obtained from the fits, we find $\theta_D\approx 140$ K. This field-independent Debye temperature is consistent with the quenching of magnetic excitations in the temperature interval of the fits and shows that the low-temperature T^3 term in the low-temperature specific heat is due to elastic phonon excitations. If we compare the departure of the data from the power-law behavior, $C/T=\gamma+\beta T^2$, in Figs. 9(a) and 9(b), a magnetic component in the specific heat becomes evident, which is suppressed at low temperatures by the 9-T magnetic field.

We remark that the Debye temperature $\theta_D\sim 140$ K obtained from the specific heat data is rather small for a rigid structure as that of an oxyborate with strong boron-oxygen bonds. On the other hand, it is consistent with the structural transition observed in the Fe ludwigite,[3] which requires soft elastic modes to occur.

A surprising feature in the present experiments is the existence of an important low-temperature linear-dependent contribution for the specific heat with a nearly field-independent coefficient γ (see above and Fig. 9). In insulating materials this linear term can be attributed to disorder. In the present case it is too large and the excellent crystallization of the samples shown by the x-ray experiments rules out this possibility. A more realistic alternative is that the present oxyborate has a metallic character and the linear specific heat term arises from itinerant electrons in the 3LLs. The value of γ we obtain is of the order of that of simple metals, like K [$\gamma_K=2.08$ mJ/(mol K^2)] or Pb [$\gamma_{Pb}=2.98$ mJ/(mol K^2)] (Ref. 24). We recall that in the Fe system, semiconducting behavior is associated with the dimerization transition,[3] as in a Peierls instability. In the Co system, since dimerization does not occur, we could expect a metallic behavior. Electron counting along the three-leg ladders leads to an extra electron for each rung of the ladder which can have an itinerant character. Transport measurements by Ivanova *et al.*[12] in a temperature range well above the magnetic transition shows thermally activated behavior of the conductivity. It remains an open question to know if this is an intrinsic behavior of the sample or is related to the eventual presence of an impurity phase.

Finally, Fig. 10 shows specific heat measurements for different applied magnetic fields in a large temperature range. Notice that the magnetic transition temperature does not shift with field, but gets rounded as this becomes very large. This rules out a simple antiferromagnetic ordering in this system.

The temperature-dependent entropy in zero field obtained from the C/T vs T curve is shown in Fig. 11. At T_N the entropy released is $S(T_N)=13.7$ J/(mol K), which is less than half of the full magnetic entropy $S=R\{2\ln[2(3/2)+1]+\ln[2.2+1]\}=36.43$ J/(mol K) expected for one Co^{3+} ($S=2$) and two Co^{2+} ($S=3/2$) per formula unit. Thus most of the entropy released up to T_N is due to the lattice. The magnetic entropy above the transition is stored in the magnetic short-range order. This is expected for a magnetic material,

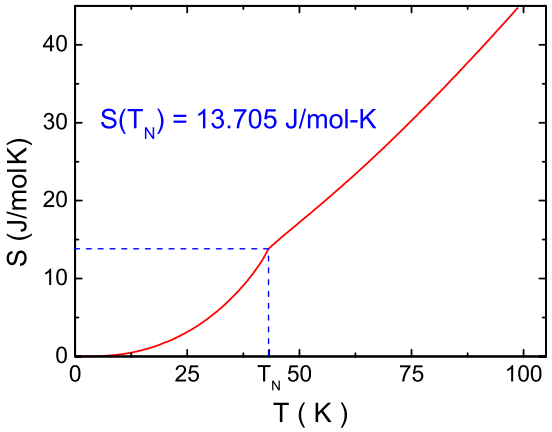

FIG. 11. (Color online) Entropy as a function of temperature obtained from the specific heat curves for the Co ludwigites.

as the present ludwigite, which consists of low-dimensional subunits in the form of three-leg ladders.

V. DISCUSSION

The oxyborates of the ludwigite type present interesting properties related to the interplay of magnetism, structural instabilities, and low dimensionality. A clear manifestation of this interplay is the existence of a dimerization instability in subunits with the form of three leg ladders that appear in the ludwigite structure. The origin of the structural transition whether magnetic or purely electronic is a matter of debate. The motivation of the present work was to study the only other known material which could throw a light in this problem. In this paper, we present a detailed crystallographic, magnetic, and thermodynamic investigation of single crystals of the Co ludwigite in an extensive temperature interval. We found, surprisingly, that in spite of very small differences in the structural properties and magnetic ions of the Co and Fe ludwigites, these materials have radical distinctions in their physical behavior. While in the Fe system the three-leg ladders become distorted in a zigzag fashion, this structural transition does not occur in the Co material. Besides $Co_3O_2BO_3$ presents a single magnetic transition where the whole sample orders magnetically. We recall that in $Fe_3O_2BO_3$ magnetic ordering occurs in two steps with a partial ordering of the Fe moments in the distorted ladders setting in first at a higher temperature.

These distinct behaviors point clearly to a strong correlation between the structural transition and the magnetic properties. Along the 3LLs in the Fe ludwigite, the electronic configuration is such that in each rung of the ladder three Fe^{3+} ions with spin $S=5/2$ share an extra electron. In the Co system this extra electron is shared by three Co^{3+} ions with spin $S=2$. There is an obvious difference that in one case we are dealing with half-integer spins. Besides that, the most important distinction is that in the Fe material the $S=5/2$ configuration corresponds to a half-filled d orbital with $L=0$, an S state. Such a state is in general associated with small magnetic anisotropy and weak coupling to the lattice due to the absence of spin-orbit coupling.

It is plausible then that in the Fe system the dimerization transition has a purely electronic origin; i.e., it is a Peierls instability as suggested in Ref. 7. In this case the partial magnetic ordering at lower temperatures arises as a *consequence* of the dimerization. For consistency, we should assume that in the Co material, spin-orbit coupling actually acts as a detriment to the Peierls transition, inhibiting the structural transition. Summing up our results implies that the connection between elastic and magnetic properties in the two known ludwigites is not simple and straightforward.

The chemical, electronic, and magnetic configurations in the ladders give rise to different mechanisms for magnetic interactions. There is the usual superexchange (SE) involving the oxygens in the edges of the tetrahedra and the double-exchange (DE) mechanism due to the polarization of the extra itinerant electron in the rungs by the local moments. These interactions are in competition, since the former is generally antiferromagnetic in the ludwigite structure, while DE favors ferromagnetism.

VI. CONCLUSIONS

We pointed out the predominance of ferromagnetic interactions in the Co ludwigite as evidenced by the large spontaneous magnetization and the reduced Curie-Weiss temperature compared to those of the Fe system. In the Fe ludwigite the magnetic structure in the ladder is such that ferromagnetically ordered rungs order antiferromagnetically at T_N (Ref. 6). The results obtained here suggest that in the Co ludwigite the magnetic ordering in the ladder is ferromagnetic in and between the rungs. In this system double-exchange prevails over superexchange interactions. This would explain the large spontaneous magnetization observed and, more important, the existence of a metallic component at very low temperatures put in evidence by the specific heat measurements. The important role of DE in the Co ludwigites could explain the breakdown of the magnetic system in domains as seen in the magnetization curves. This a well-established feature of systems where DE is dominant.[25] While these results shed light on the magnetism in the ladders, they leave unanswered the question of why the dimerization transition does not occur in the Co ludwigite—specially, since theoretical work has shown that DE can give rise to dimerization. The main difficulty of theories which attribute a magnetic origin for the structural transition is of course that these transitions in $Fe_3O_2BO_3$ occur at different temperatures.

We have presented in this paper an extensive experimental study of the Co ludwigite material. Similar studies have been previously carried out in a Fe ludwigite. These are only two known homometallic ludwigites. In view of the similar structural parameters and ionic configurations, we expected to find similar properties in both materials with eventual differences in nonuniversal quantities such as the temperatures of the structural and magnetic instabilities. The results, however, turned out to be surprising and open a range of possibilities. Clearly an understanding of the differences in

physical behavior of these ludwigites can throw light on the nature of the several competing mechanisms which determine the physical properties of mixed valence materials, especially in low dimensions. The single crystals we obtain are two small for direct measurement of the electrical properties. We expect to circumvent this difficulty in the near future The transport measurements can clarify whether the high resistances found in Ref. 12 is due to impurity phases or an intrinsic phenomenon. Hopefully our results will motivate further theoretical work in these interesting materials.

ACKNOWLEDGMENTS

Support from the Brazilian agencies CNPq and FAPERJ is gratefully acknowledged.

*mucio@if.uff.br

[1] M. A. Continentino, J. C. Fernandes, R. B. Guimarães, B. Boechat, and A. Saguia, *Frontiers in Magnetic Materials* (Springer, Berlin, 2005), p. 385.

[2] M. Angst, P. Khalifah, R. P. Hermann, H. J. Xiang, M.-H. Whangbo, V. Varadarajan, J. W. Brill, B. C. Sales, and D. Mandrus, Phys. Rev. Lett. **99**, 086403 (2007); I. Leonov, A. N. Yaresko, V. N. Antonov, J. P. Attfield, and V. I. Anisimov, Phys. Rev. B **72**, 014407 (2005); I. Leonov, A. N. Yaresko, V. N. Antonov, J. P. Attfield, and V. I. Anisimov, *ibid.* **74**, 176402 (2006).

[3] M. Mir, R. B. Guimarães, J. C. Fernandes, M. A. Continentino, A. C. Doriguetto, Y. P. Mascarenhas, J. Ellena, E. E. Castellano, R. S. Freitas, and L. Ghivelder, Phys. Rev. Lett. **87**, 147201 (2001); A. P. Douvalis, A. Moukarika, T. Bakas, G. Kallias, and V. Papaefthymiou, J. Phys.: Condens. Matter **14**, 3303 (2002); J. A. Larrea, D. R. Sánchez, E. M. Baggio-Saitovitch, J. C. Fernandes, R. B. Guimarães, M. A. Continentino, and F. J. Litterst, J. Magn. Magn. Mater. **226-230**, 1079 (2001).

[4] R. B. Guimarães, M. Mir, J. C. Fernandes, M. A. Continentino, H. A. Borges, G. Cernichiaro, M. B. Fontes, D. R. S. Candela, and E. Baggio-Saitovitch, Phys. Rev. B **60**, 6617 (1999).

[5] J. Larrea J., D. R. Sanchez, F. J. Litterst, E. M. Baggio-Saitovitch, J. C. Fernandes, R. B. Guimarães, and M. A. Continentino, Phys. Rev. B **70**, 174452 (2004).

[6] P. Bordet, E. Suard, J. Dumas, M. Avignon, J.-L. Tholence, M. A. Continentino, and M. Mir, Acta Crystallogr. **61**, C57 (2005).

[7] A. Latgé and M. A. Continentino, Phys. Rev. B **66**, 094113 (2002).

[8] M. Whangbo, H.-J. Koo, J. Dumas, and M. A. Continentino, Inorg. Chem. **41**, 2193 (2002).

[9] E. Vallejo and M. Avignon, Phys. Rev. Lett. **97**, 217203 (2006).

[10] R. Norrestam, K. Nielsen, I. Sotofte, and N. Thorup, Z. Kristallogr. **189**, 33 (1989).

[11] Zi-Xiang Huang, Wen-Dan Cheng, and Hao Zhang, Chin. J. Struct. Chem. **20**, 97 (2001).

[12] N. B. Ivanova, A. D. Vasil'ev, D. A. Velikanov, N. V. Kazak, S. G. Ovchinnikov, G. A. Petrakovskii, and V. V. Rudenko, Phys. Solid State **49**, 651 (2007).

[13] J. L. C. Rowsell, N. J. Taylor, and L. F. Nazar, J. Solid State Chem. **174**, 189 (2003).

[14] Enraf-Nonius, computer code COLLECT, Nonius BV, Delft, The Netherlands, 1997–2000.

[15] Z. Otwinowski and W. Minor, in *Methods in Enzymology*, edited by C. W. Carter, Jr. and R. M. Sweet (Academic Press, New York, 1997), p. 276.

[16] P. Coppens, L. Leiserowitz, and D. Rabinovich, Acta Crystallogr. **18**, 1035 (1965).

[17] G. M. Sheldrick, computer code SHELXS97, a program for crystal structure solution (release 97-2), Institüt für Anorganische Chemie der Universität, Tammanstrasse 4, D-3400 Göttingen, Germany, 1998.

[18] G. M. Sheldrick, computer code SHELXL97, a program for crystal structure refinement (release 97-2), Institüt für Anorganische Chemie der Universität, Tammanstrasse 4, D-3400 Göttingen, Germany, 1998.

[19] L. J. Farrugia, J. Appl. Crystallogr. **32**, 837 (1999).

[20] L. J. Farrugia, J. Appl. Crystallogr. **30**, 565 (1997).

[21] G. Bergherhoff, M. Berndt, and K. Brandenburg, J. Res. Natl. Inst. Stand. Technol. **101**, 221 (1996).

[22] R. M. Wood and G. J. Palenik, Inorg. Chem. **37**, 4149 (1998); D. C. de Freitas, M.Sc. thesis, Universidade Federal Fluminense, 2007.

[23] J. C. Fernandes, R. B. Guimarães, M. A. Continentino, L. Ghivelder, and R. S. Freitas, Phys. Rev. B **61**, R850 (2000).

[24] C. Kittel, *Introduction to Solid State Physics*, 5th ed. (Wiley, New York, 1976), p. 167.

[25] D. J. Garcia, K. Hallberg, C. D. Batista, M. Avignon, and B. Alascio, Phys. Rev. Lett. **85**, 3720 (2000); H. Aliaga, B. Normand, K. Hallberg, M. Avignon, and B. Alascio, Phys. Rev. B **64**, 024422 (2001).